



# Dynamic fracture of the AISI 1045 steel cylinders under internal blast loading\*

1<sup>st</sup> Y Ma<sup>1</sup> 2<sup>nd</sup> Y He<sup>\*1</sup> 3<sup>rd</sup> CT Wang<sup>\*1</sup> 4<sup>th</sup> Y He<sup>1</sup> 5<sup>th</sup> ZP Guo<sup>1</sup> 6<sup>th</sup> X B Hu<sup>1</sup>

<sup>1</sup>ZNDY of Ministerial Key Laboratory, Nanjing University of Science and Technology, Nanjing, China, 210094

Email: mayue68@njust.edu.cn(Y Ma); Yonghe1964@163.com(Y He); ctwang@njust.edu.cn(CT Wang).

## ABSTRACT

Dynamic fracture failure of the AISI 1045 steel cylinders with variable depth grooves under internal blast loading was investigated. Lateral and longitudinal grooves were curved on the wall of steel cylinders along with radial direction. All grooves have a V-shape with 20° angle. After blast, the morphology of fragments recovered by multi-layer wooden plank showed relative consistency. Microstructure in cross and longitudinal section of the fragments was examined by scanning electron microscope (SEM). The microstructure observation suggested that there were some undeveloped shear bands and the dynamic fracture modes were similar in the all tests but the different fracture mode in two directions. Relevant numerical simulation by LS-DYNA were carried out to analyze the expanding and fracture process of cylinders under internal blast loading. Numerical results have acceptable agreement with experiment results. The mass loss rate of shell after explosion is negatively correlated with the depth of grooves.

## I. INTRODUCTION

The dynamic fracture failure of explosive cylinder shell is very important for the design of warhead. Under detonation loading, the inner wall of the cylinder shell will be affected by high temperature and high pressure which will quickly conduct to the whole shell wall thickness. The whole shell expands and breaks rapidly under the conditions of high temperature, high pressure, high strain and high strain rate, and the process is short and intense. So it's quite complicated. So far, scholars have focused on fracture mechanism, fracture strain, fracture stress, fracture size and fracture velocity.

In this paper, AISI 45 steel is used as shell material, and v-shaped groove is carved symmetrically inside and outside, and the groove angle is 20 degrees. The circumferential and axial fracture processes of the shell under internal blast loading are studied.

## II. EXPERIMENT

### A. Experiment set-up

The specimen used in the test was made from AISI45 steel without any heat treatment. Its inner diameter, wall thickness, height is 62mm, 10mm, 120mm, respectively. V-shaped grooves are symmetrically carved on the inner and outer walls of the shell. The angle of the groove is 20 degrees. The physical specimens used in the test are shown in figure 1. In the test, the end-point center detonation mode was adopted. The shell was placed vertically on the surface of cement pier, surrounded by wood boards at a distance of 1.5m. The boards are 20mm thick, with 15 layers in each direction. The experimental arrangement is shown in figure 2.

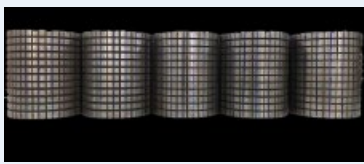


Fig. 1. The physical specimens used in the test



Fig. 2. the experimental set-up

### B. Experiment results

After blast, fragments were recovered from the wood boards. The recovered fragments are shown in the figure 3a-c.

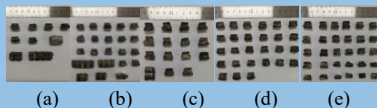


Fig. 3. Recovered fragments with variable groove depth: (a) grooves depth=2.5mm; (b) grooves depth=3.0mm; (c) grooves depth=3.5mm; (d) grooves depth=4.0mm; (e) grooves depth=4.5mm.

Defining that the ideal fragment mass is the total mass of the shell divided by the number of pre-control fragments, the mass loss rate of fragments after explosive loading of the shell in various experiment was obtained under the condition that the recovered fragments were weighed. The relationship between the mass loss rate and the depth of notches is shown in the figure 4.

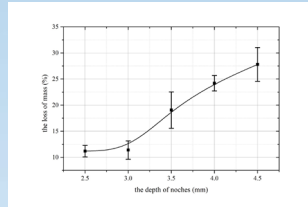


Fig. 4. The mass loss rate with variable groove depth

## III. SIMULATION

### A. Method

The simulation model is shown in the figure 5.

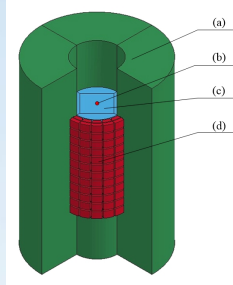


Fig. 5. Graph simulation model:(a) air; (b) initial detonation point; (c) charge; (d) shell.

The shell material is AISI45 steel, which is described by Johnson-Cook (JC) material model and Gruneisen state equation. The detonation of explosive, with high explosive detonation model (\*MAT\_HIGH\_EXPLOSIVE\_BURN), is described by JWJ equation. Air with null materials (\*MAT\_NULL) model is described by linear polynomial equation of state (\*EOS\_LINEAR\_POLYNOMIAL). Their parameter values are shown in table 1-3.

Table 1. The parameters of Johnson-Cook (JC) material model of AISI 45 steel

$\rho_0/(g \cdot cm^{-3})$	A/MPa	B/MPa	n	C
7.85	507	320	0.28	0.064
m	D1	D2	D3	D4
1.06	0.10	0.76	1.57	0.005

D5	$C_0/(km \cdot s^{-1})$	$S_f$	$\gamma_0$
-0.84	4.569	1.49	2.17

Table 2. The parameters of high explosive

$\rho_0/(g \cdot cm^{-3})$	D	PCJ/GPa	A/GPa	B/GPa
1.78	8425	29.7	854.5	20.49

R1	R2	$\omega$	A/GPa	$\sigma_y/GPa$
4.6	1.35	0.25	3.54	0.2

Table 3. The parameters of air

$\rho_0/(g \cdot cm^{-3})$	C0	C1	C2
0.00129	0	0	0
C3	C4	C5	C6
0	0.4	0.4	0

### B. Results

The dispersion field of fragments at different time can be obtained by numerical simulation, as shown in Figure 6 (an example of the simulation result of 4.5 groove depth).



Fig. 6. The diagram of dispersion field from numerical simulation: (a) front view; (b) isometric view.

The distribution of fragmentation velocity along the axial direction is shown in the Figure 7.

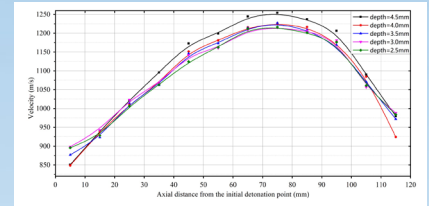


Fig. 7. Fragment velocity along the axial direction

The expansion of the shell at different times is shown in the Figure 8.

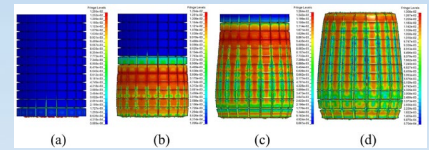


Fig. 8. The expansion process of the shell at different times: (a) 5μs; (b) 10μs; (c) 15μs; (d) 20μs.

## IV. DISCUSSION

According to Ref [1], there are mainly two fracture modes: shear fracture and tension-shear mixed fracture mode. After polishing the recovered fragments, SEM was used for metallographic observation. The microstructure of the cross section shows the great consistency(Figure 9-10).

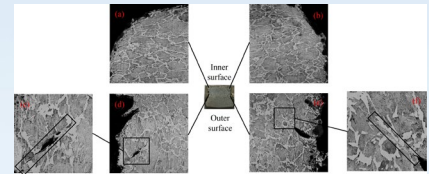


Fig. 9. The metallographic image of the cross section (groove depth =3.5mm): (a) inner corner of left side; (b) inner corner of right side; (c) (d)the shear crack of left side; (e); (f) the shear band of left side.

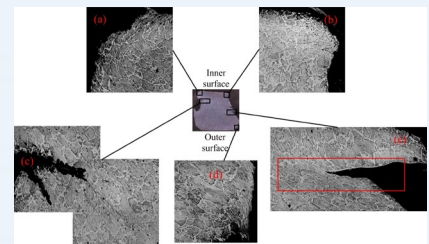


Fig. 10. The metallographic image of the longitudinal section (groove depth =2.5mm): (a) inner corner of left side; (b) inner corner of right side; (c) the crack of left side; (d)the deformation of external corner of right side;(e)shear crack.

## V. CONCLUSION

Based on the above work, the following conclusions are drawn:

(1)The circumferential fracture mode of the shell with internal and external grooves is mainly tensile-shear mixed fracture mode, and the shear crack starts in the inner wall and the tensile crack starts in the outer wall. The fracture modes on both sides of the circumferential rupture are the same;

(2)The axial fracture mode of the shell with internal and external grooves is mainly tensile-shear mixed fracture mode, but the fracture mode on both sides of the fragments is not same in the axial direction. The side near the starting point end under detonation pressure germinates the initial shear crack at the bottom of the internal groove, then tensile crack at the bottom of the external groove initiates. On the other side, it is tensile fracture near the inside of the fragment;

(3) The mass loss rate of the shell is positively correlated with the groove depth.